

# ULRR

## Enhanced photocatalytic degradation of acetaminophen from wastewater using WO<sub>3</sub>/TiO<sub>2</sub>/SiO<sub>2</sub> composite under UV–VIS irradiation

|               |   |
|---------------|---|
| Item Type     | Article   |
| Authors       | Yanyan, Lin;Kurniawan, Tonni Agustiono;Ying, Z;Albadarin, Ahmad B.;Walker, Gavin                                    |
| Citation      | Journal of Molecular Liquids;243, pp. 761-770   |
| Publisher     | Elsevier  |
| Download date | 2026-05-14 01:50:15   |
| Item License  | <a href="https://creativecommons.org/licenses/by-nc-sa/1.0/">https://creativecommons.org/licenses/by-nc-sa/1.0/</a> |
| Link to Item  | <a href="https://hdl.handle.net/10344/6145">https://hdl.handle.net/10344/6145</a>                                   |

## Accepted Manuscript

Enhanced photocatalytic degradation of acetaminophen from wastewater using WO<sub>3</sub>/TiO<sub>2</sub>/SiO<sub>2</sub> composite under UV–VIS irradiation

Lin Yanyan, Tonni Agustiono Kurniawan, Z. Ying, Ahmad B. Albadarin, Gavin Walker



PII: S0167-7322(17)33881-3  
DOI: doi: [10.1016/j.molliq.2017.08.092](https://doi.org/10.1016/j.molliq.2017.08.092)  
Reference: MOLLIQ 7800

To appear in: *Journal of Molecular Liquids*

Received date: 27 July 2017  
Revised date: 16 August 2017  
Accepted date: 17 August 2017

Please cite this article as: Lin Yanyan, Tonni Agustiono Kurniawan, Z. Ying, Ahmad B. Albadarin, Gavin Walker , Enhanced photocatalytic degradation of acetaminophen from wastewater using WO<sub>3</sub>/TiO<sub>2</sub>/SiO<sub>2</sub> composite under UV–VIS irradiation, *Journal of Molecular Liquids* (2017), doi: [10.1016/j.molliq.2017.08.092](https://doi.org/10.1016/j.molliq.2017.08.092)

This is a PDF file of an unedited manuscript that has been accepted for publication. As a service to our customers we are providing this early version of the manuscript. The manuscript will undergo copyediting, typesetting, and review of the resulting proof before it is published in its final form. Please note that during the production process errors may be discovered which could affect the content, and all legal disclaimers that apply to the journal pertain.

**Enhanced photocatalytic degradation of acetaminophen from wastewater using****WO<sub>3</sub>/TiO<sub>2</sub>/SiO<sub>2</sub> composite under UV-VIS irradiation**

**Lin Yanyan<sup>a</sup>; Tonni Agustiono Kurniawan<sup>a\*</sup>; Z. Ying<sup>a</sup>; Ahmad B. Albadarin<sup>b</sup>, Gavin Walker<sup>b</sup>**

<sup>a</sup>College of Ecology and Environment, Xiamen University, Xiamen 361102

Fujian Province, PR China Tel: (+86) 592-1565-980 Fax: (+86) 592-2185889

\*Email: tonni@xmu.edu.cn (corresponding author)

<sup>b</sup>Department of Chemical and Environmental Sciences, Bernal Institute, University of Limerick, Limerick, Ireland

**Abstract**

This study investigates the photocatalytic degradation of acetaminophen (Ace) from synthetic wastewater by individual  $\text{TiO}_2$ ,  $\text{TiO}_2/\text{SiO}_2$  and/or  $\text{WO}_3/\text{TiO}_2/\text{SiO}_2$  composite under UV-VIS illumination. To characterize changes in their morphology and crystal structures before and after treatment, X-ray diffraction (XRD), Fourier transform infrared spectroscopy (FTIR), DRS UV-VIS absorption spectra, Brunauer-Emmer-Teller (BET) and scanning electron microscopy (SEM) techniques were used. The effects of varying loading ratios of the  $\text{WO}_3$  on the  $\text{TiO}_2/\text{SiO}_2$  composite for Ace degradation were studied. Operating parameters such as initial concentration, reaction time, dose of photocatalyst and pH were tested. Degradation by-products were also presented. It is found that the photodegradation performance of the  $\text{WO}_3/\text{TiO}_2/\text{SiO}_2$  composite as a photocatalyst in this study could be enhanced by optimizing the loading ratio of the  $\text{WO}_3$ . About 3% (w/w) of  $\text{WO}_3/\text{TiO}_2/\text{SiO}_2$  was found to improve the degradation of Ace from 33% to 95% at the same initial concentration of 5 mg/L. The resulting oxidation by-products included hydroquinone and 1,4-benzoquinone. Under the same conditions, the result of photocatalytic degradation by the 3% (w/w) of  $\text{WO}_3/\text{TiO}_2/\text{SiO}_2$  composite was significantly higher (95%) than that by the individual  $\text{TiO}_2/\text{SiO}_2$  (42%) and/or by the  $\text{TiO}_2$  alone (33%). Under optimized conditions (1.5 g/L; 3% (w/w) of  $\text{WO}_3/\text{TiO}_2/\text{SiO}_2$  composite; pH 9; 4 h of reaction time), 95% of Ace removal with an initial concentration of 5 mg/L could be attained. However, the treated effluents still could not meet the discharge standard of less than 0.2 mg/L set by China's and US legislation. This indicates that further subsequent treatment like biological processes is still necessary for completing the removal of target pollutant from the wastewater samples.

*Keywords:* Advanced oxidation process (AOP); Pharmaceuticals and personal care products; endocrine-disrupting compounds (EDC); Titanium composite; Wastewater treatment

## 1. Introduction

Pharmaceuticals and personal care products (PPCPs) such as therapeutic drugs, hormones and skin care products have attracted global environmental concerns in recent decades [1-2]. With the improving living standards of people in recent years, the production and consumption of PPCPs has increased in China. As a result, a large amount of residual PPCPs is discharged into the aquatic environment, causing adverse impacts on the environment and public health [3].

Among the various PPCPs, acetaminophen (Ace) is one of the widely used pain relief drugs. The pollutant is often found in the municipal sewage effluents with varying trace concentrations in different parts of the world including the US, Greece and China [3-5]. Furthermore, Ace is toxic to living organisms because it cannot be completely metabolized in human body. Considering its potential risks when it accumulates through food chains, the pollutant has to be completely eliminated from wastewater.

In recent years, various technologies have been developed and tested in laboratory systems or pilot plants to remove various PPCPs from wastewater [6-8]. The use of semi-conductor composites as a photocatalyst in advanced oxidation process (AOP) has emerged as one of the most promising options due to the generation of hydroxyl radicals ( $\cdot\text{OH}$ ) [9-11]. The  $\cdot\text{OH}$ , with a high oxidation potential of 2.80 V (Reaction (1)), can indiscriminately react with target pollutants in solutions for a complete degradation.



Due to its low-cost and chemical stability, semi-conductor material like  $\text{TiO}_2$  has been commonly used in recent years [12]. However, the  $\text{TiO}_2$  has a limited utilization efficiency of visible

spectrum (only 4%) due to its wide band gap (3.2 eV) [13]. Consequently, its rapid recombination of photo-reacted electron-hole pairs and a poor photo-induced reaction performance leads to a low photocatalytic efficiency [14-15]. As a result, a number of UV lamps are required for maximizing the removal of target pollutants during treatment, thus increasing its operational costs.

To maximize the utilization of visible light, an ideal photocatalyst should work within the range of visible light and a band-gap of less than 3.0 eV is required [16]. For this reason, various semi-conductors such as CeO<sub>2</sub>, CuO, WO<sub>3</sub>, SnO<sub>2</sub> and SiO<sub>2</sub> have been employed by integrating them with TiO<sub>2</sub> in the form of composites [17-19].

Silicon dioxide (SiO<sub>2</sub>) is one of the most promising materials, as it does not interfere with any absorption within the UV range. With this characteristic, SiO<sub>2</sub> can work as a dopant either to enhance photocatalytic activities under a visible light or to extend the absorption band to reach the visible spectrum [20-21]. In addition, this material could improve the thermal stability of the composite and enhance its surface activity or surface area [14, 22] when it is activated with TiO<sub>2</sub> during their formation as a composite.

Apart from the SiO<sub>2</sub>, tungsten trioxide (WO<sub>3</sub>) has unique properties because of its optical, chemical and electrochemical factors [23]. Compared to the TiO<sub>2</sub>, the WO<sub>3</sub> has not only a relatively lower band-gap energy (2.8 eV), but also the capability of absorbing a wider range of visible spectrum than the former. Moreover, the WO<sub>3</sub> has gained considerable attention due to its excellent photo-corrosion resistance and chemical stability toward continuous contact to solar light illumination. In their preliminary studies, Hunge and Riboni *et al.* [24-25] reported that the combination of both the TiO<sub>2</sub> and the WO<sub>3</sub> have enhanced the photocatalytic reactions and their stability, as their integration into a semi-conductor composite might improve the charge separation by capturing photo-generated electrons [25].

Considering that the search for semi-conductor materials for water technology has intensified in recent years, to the best of our knowledge, so far none has reported the technical feasibility of the  $\text{WO}_3/\text{TiO}_2/\text{SiO}_2$  (WTS) composite for photocatalytic degradation. The ideal photocatalyst should be visible-light active and maximize its lifetime for practical use. The incorporation of the WTS composite not only provides an eco-friendly approach to remove PPCPs from wastewater, but also maximizes the advantages of integrating both  $\text{SiO}_2$  and  $\text{WO}_3$  as a composite, while simultaneously addressing the limitation of  $\text{TiO}_2$ . This work represents an original contribution to the field of study with respect to the scope of the composite from synthesis, characterization and regeneration to its application for photodegradation of Ace from wastewater, while understanding their physico-chemical interactions in liquid solutions. From practical points of view, a stable WTS in the form of a composite may have a favorable photocatalytic activity because of its larger surface area, particle size and visible light utilization efficiency.

The laboratory studies reported in this article investigates the technical applicability of Ace degradation from wastewater by individual  $\text{TiO}_2$ ,  $\text{TiO}_2/\text{SiO}_2$ , and/or  $\text{WO}_3/\text{TiO}_2/\text{SiO}_2$  under UV-VIS illumination. To characterize changes in their morphology and crystal structure properties before and after treatment, advanced techniques such as X-ray diffraction (XRD), Fourier transform infrared spectroscopy (FTIR), DRS UV-VIS absorption spectra, Brunauer-Emmer-Teller (BET) and scanning electron microscopy (SEM) techniques were used. The effects of different loading ratios of the  $\text{WO}_3$  on the  $\text{TiO}_2/\text{SiO}_2$  composite for Ace photocatalytic degradation were studied. Operational parameters such as initial concentration, reaction time, dose of photocatalyst and pH were investigated. Degradation by-products, resulting from the treatment, are also presented.

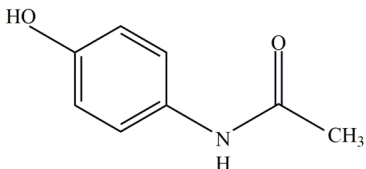
## 2. Materials and Methods

### 2.1. Materials

Chemicals such as tetrabutyl orthotitanate ( $\text{Ti}[\text{OC}(\text{CH}_3)_3]_4$ , TBOT, >98%), tetraethyl orthosilicate ( $\text{Si}(\text{OC}_2\text{H}_5)_4$ , TEOS, >98%), sodium tungstate ( $\text{Na}_2\text{WO}_4$ , >99.5%) were obtained from Sigma–Aldrich (China). Other chemicals such as Ace (Table 1) were of analytical grade and supplied by Acros (New Jersey, USA). They were used as-received without further purification. The initial pH of Ace solution was adjusted by 1.0 M NaOH and/or HCl and determined using a pHmeter (model Mettler FE 20, Switzerland). All of the standard solutions were freshly prepared from a stock solution using deionized (DI) water.

**Table 1**

Characteristics of acetaminophen.

| Pollutant     | Molecular formula                 | $\lambda_{\text{max}}$ (nm) | Molar mass (g/mol) | $\text{pH}_{\text{zpc}}$ | pKa | Molecular structure  |
|---------------|-----------------------------------|-----------------------------|--------------------|--------------------------|-----|--|
| Acetaminophen | $\text{C}_8\text{H}_9\text{NO}_2$ | 243                         | 151.16             | 6.4                      | 9.5 |  |

### 2.2. Methods

#### 2.2.1 Synthesis of photocatalysts

The  $\text{TiO}_2/\text{SiO}_2$  was synthesized based on the sol-gel method [26]. Initially, about 0.75 mL of TEOS was proportionally mixed with  $\text{C}_2\text{H}_5\text{OH}$  and deionized water, and then magnetically stirred

for 1 h. Afterward, a predetermined amount of HCl was added into the same solution and kept stirred for another 4 h. A separate solution of TBOT, C<sub>2</sub>H<sub>5</sub>OH and HCl was magnetically stirred for 5 h at the same time. Then, the TEOS and the TBOT mixture were combined and subsequently stirred for 3 h to complete a hydrolysis process. The required amounts of each component were dispersed to obtain a Si/Ti molar ratio of 1:9 after mixing.

A predetermined amount of Na<sub>2</sub>WO<sub>4</sub>, used as a precursor of the WO<sub>3</sub>, was added into the TiO<sub>2</sub>/SiO<sub>2</sub> solution and then vigorously stirred for 1 h to obtain 1, 3, 5 and 7% (w/w) of the WTS composites respectively. Then, the obtained mesophase was transferred into a chamber aging for 12 h. After calcination at 500°C for 3 h, the samples were collected and cooled down at ambient temperature. All types of WTS composites were stored in a desiccator until required for further use. The final products were denoted as 1WTS, 3WTS, 5WTS and 7WTS respectively, in which the first number corresponded to the weight ratios of the WO<sub>3</sub> in their composites.

### 2.2.2. Characterization of WO<sub>3</sub>/TiO<sub>2</sub>/SiO<sub>2</sub> composite

The X-ray powder diffraction (model Rigaku Ultima IV, Tokyo, Japan) method was recorded to measure the crystal structure of the composites in their powder form. It operated at 40 kV and 30 mA. Varying diffraction angles (2θ) from 20° to 80° at a scanning speed of 10°/min were employed. The FT-IR (IS50, Thermo, New York, USA) analyses were undertaken to identify certain chemical bond vibration of the composites. The diffuse reflectance spectra (DRS) UV-VIS absorptions were recorded through a UV-VIS spectrophotometer (model Shimadzu 2600, Tokyo, Japan) to evaluate the band-gap of the obtained composites with wavelengths from 350 to 550 nm. The specific area and porosity of the samples were calculated by using a BET nitrogen adsorption isotherm method (model Nova 1200e, Massachusetts, US). The surface morphologies of the obtained composites were analyzed using a

scanning electron microscope (model ZEISS SIGMA, Jena, Germany), which operated at 15 kV.

### 2.2.3 Photocatalytic degradation

Photodegradation of Ace using individual  $\text{TiO}_2$ ,  $\text{TiO}_2/\text{SiO}_2$ , and/or WTS composites was undertaken in a photoreactor (Fig. 1). A full waveband xenon lamp with a power of 500 W coupled with a cutoff filter ( $800 \text{ nm} > \lambda > 200 \text{ nm}$ ) was installed inside the reactor. The Ace solution with an initial concentration of 10 mg/L and 0.5 g of photocatalyst were prepared in a suspension (0.5 L) onto a cylindrical reactor with a diameter of 10 mm and height of 220 mm. All reactants were magnetically stirred until the formation of a homogenous suspension of the photocatalyst.

To enhance Ace removal, operational parameters such as dose of photocatalysts, initial concentration of Ace, reaction time and pH were optimized. The overall photocatalytic reaction ran for 4 h and treated effluents were collected periodically for determining the remaining Ace concentration. At each sampling, the effluents were filtered using Millipore filter papers (pore size  $0.22 \mu\text{m}$ ) to remove the residual photocatalyst. The resulting oxidation by-products were detected by using a GC/MS (Hewlett Packard, HP 6890) equipped with a mass selective detector (Hewlett Packard, HP 6890).

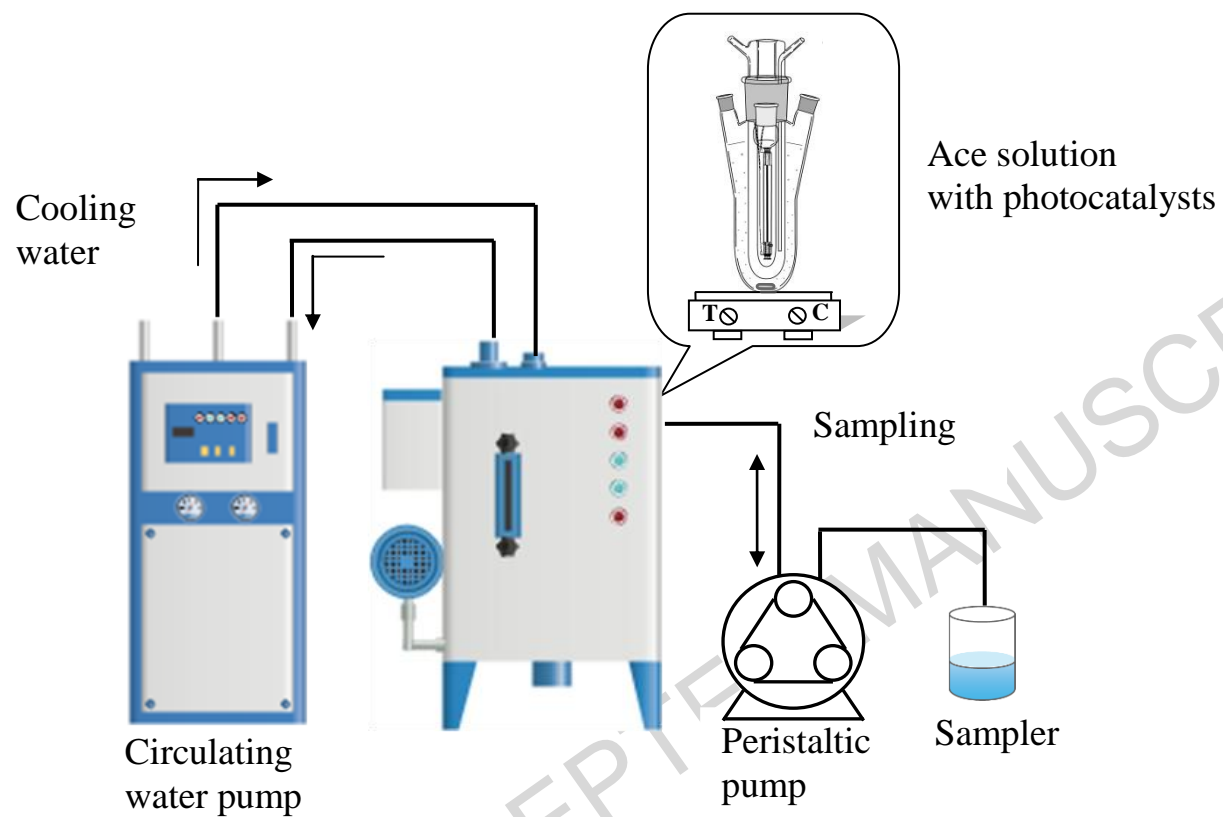


**Fig. 1.** Scheme of photoreactor used for Ace photodegradation.

### 2.5. Chemical analysis of Ace

The remaining concentration of Ace after treatment was analyzed using a UV-VIS spectrophotometer (model Mapada UV1800, Shanghai, China) at its maximum absorption wavelength ( $\lambda=243$  nm). The removal efficiency of Ace ( $\eta(\%)$ ) is defined as:

$$\eta (\%) = \left[ \frac{C_0 - C_e}{C_0} \right] \times 100\% \quad (2)$$

where  $C_0$  and  $C_e$  represent the initial and the equilibrium Ace concentration, respectively.

### 2.6. Reuse of spent photocatalysts

In order to test its reusability and stability, regeneration studies were carried out using the same 3% (w/w) of the spent WTS. After being saturated, suspension was centrifuged, and the photocatalyst was separated from it. Afterwards, the residual photocatalyst was repeatedly washed for several times, dried at 80 °C, then regenerated.

### 2.7 Statistical analysis

In order to ensure the accuracy and replicability of the obtained data, the same experiments were repeated at least in triplicate under the same operating conditions, and the average value of the data was presented. The coefficient of variation for the obtained data was less than 5%. If the relative error of the Ace removal rate exceeded 5%, an identical fourth run would be conducted until the error was within the acceptable range. All statistical tests were carried out using SPSS 19.0 (Window Version) with a confidence interval of 95%. Differences were considered statistically significant when  $p \leq 0.05$ .

### 3. Results and Discussion

#### 3.1. Characterization of $WO_3/TiO_2/SiO_2$ composite

##### 3.1.1. X-ray diffraction (XRD) analysis

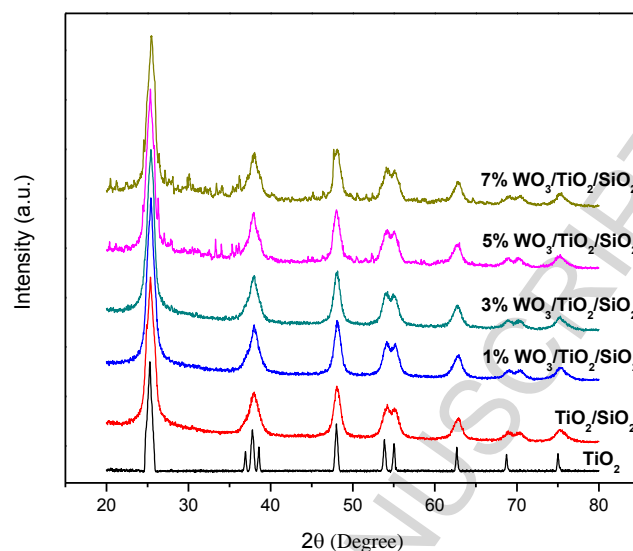


**Fig. 2.** XRD patterns for  $TiO_2$ ,  $TiO_2/SiO_2$  and varying  $WO_3$  loading ratios in  $WO_3/TiO_2/SiO_2$  composites.

Fig. 2 presents the crystal structures of the  $TiO_2$  and the WTS composite based on the XRD analyses. There was no diffraction peak observed for the  $SiO_2$ , as the material existed in an amorphous state. Consequently, its diffraction peaks could not be detected by the XRD analysis [27]. The peaks of the obtained composites at 25.5°, 37.8°, 48.0°, 53.8°, 55.0°, 63.0° and 68.7° reveal the typical locations of the  $TiO_2$  peaks (PDF card 21-1272, JCPDS). Based on the location of  $TiO_2$ , it is inferred that the  $TiO_2$  in all of the composites existed in the form of anatase phase, regardless of their  $WO_3$  content (1-7% (w/w)) [28].

The predominant peaks of the  $TiO_2/SiO_2$  composite also exhibited consistent positions, while demonstrating different peaks' intensity. This result suggests that the addition of the  $SiO_2$  into the composite did not affect the lattices structure of the  $TiO_2$ , thus maintaining an efficient photocatalytic activity. On the other hand, this indicates that the presence of the Si atom inhibited

the transformation of the Ti from anatase to rutile phases, even though being calcined at 500°C for 3 h. Nasirian *et al.* [28] found that a small amount of TiO<sub>2</sub> would be converted to its rutile phase at 500°C. This result is in agreement with that of a study undertaken by Qourzal *et al.* [21], who reported that the presence of silica prevented the transformation of TiO<sub>2</sub> from anatase to rutile phase.

After depositing the WO<sub>3</sub> on the TiO<sub>2</sub>/SiO<sub>2</sub>, the peaks and intensity of the WTS composite were identical to those of the TiO<sub>2</sub>/SiO<sub>2</sub>, especially the 1WTS and the 3WTS since the WO<sub>3</sub> might have been incorporated into the lattices of TiO<sub>2</sub> in their composite [21]. When the loading ratio of the WO<sub>3</sub> reached 5%, the XRD patterns of the 5WTS and the 7WTS showed impurity peaks between the range of 25° and 40°. As a result, the excessive WO<sub>3</sub> could not enter into the lattices of the TiO<sub>2</sub>.

### 3.1.2. FTIR spectra analysis

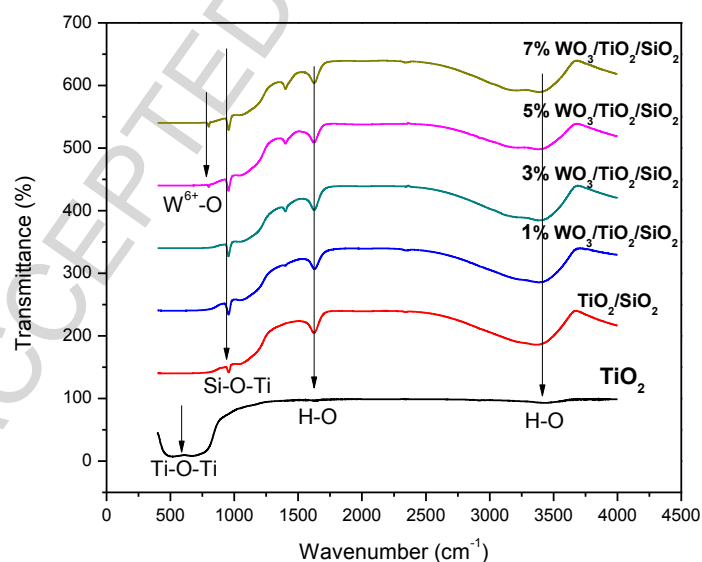


**Fig. 3.** FT-IR spectra of TiO<sub>2</sub>, TiO<sub>2</sub>/SiO<sub>2</sub> and varying WO<sub>3</sub> loading ratios in WO<sub>3</sub>/TiO<sub>2</sub>/SiO<sub>2</sub> composites

FTIR studies were used to detect and identify functional groups of the composites before and after their incorporation with the SiO<sub>2</sub> and the WO<sub>3</sub>. As depicted in Fig. 3, the band of the TiO<sub>2</sub> within 500-800 cm<sup>-1</sup> corresponds to the Ti-O-Ti vibrations bonds [29]. The characteristic peaks at 3422 cm<sup>-1</sup> both for the TiO<sub>2</sub>/SiO<sub>2</sub> and for the WTS are due to the stretching of the O-H bond of the absorbed water and the OH- groups of the composites [29-30].

Compared to the as-received TiO<sub>2</sub>, the TiO<sub>2</sub>/SiO<sub>2</sub> composite shows a weak peak at 1059 cm<sup>-1</sup> due to the asymmetric stretching frequency of the Si-O bond, while the peaks at 955 cm<sup>-1</sup> for all the composites are associated with the asymmetric Si-O-Ti vibration. This confirms that the Si atom had been incorporated into the framework of Ti. These findings confirm those of the studies undertaken by Guo *et al.* [29] and Qourzal *et al.* [21], who also demonstrated the Si-O-Ti vibration at the range of 930-960 cm<sup>-1</sup>.

In addition, significant peaks for the WO<sub>3</sub> could not be observed until the weight ratio of the WO<sub>3</sub> reached 5%. The slightly absorption peak of the WO<sub>3</sub> at 800 cm<sup>-1</sup> (Fig. 3) corresponds to the symmetric mode of W<sup>6+</sup>-O stretching vibrations [25]. This finding supports the studies undertaken by Ismail *et al.* [31], who found that there were no WO<sub>3</sub> peaks until the molar ratio between WO<sub>3</sub> and TiO<sub>2</sub> reached 5%.

### 3.1.3. DRS UV-VIS spectra

To understand the efficiency of the obtained photocatalysts for the photodegradation of organic pollutants, it is essential to improve their visible light utilization. Fig. 4 presents the UV-VIS spectra of the TiO<sub>2</sub>, TiO<sub>2</sub>/SiO<sub>2</sub> and WTS composites.

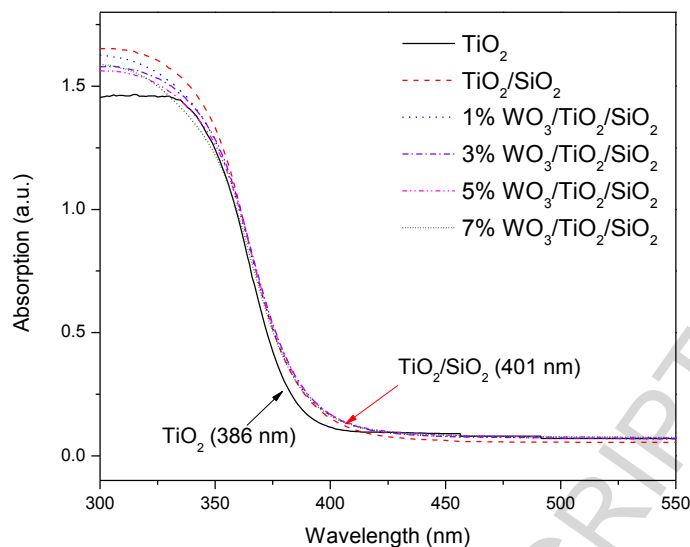


**Fig. 4.** Diffuse reflectance of UV-VIS spectra for TiO<sub>2</sub>, TiO<sub>2</sub>/SiO<sub>2</sub> and varying WO<sub>3</sub> loading ratios in WO<sub>3</sub>/TiO<sub>2</sub>/SiO<sub>2</sub> composites.

Previous reports suggested that no absorption was observed either in UV or in visible regions for the SiO<sub>2</sub> alone [27]. As compared to the pure TiO<sub>2</sub>, a noticeable shift of the absorption spectrum to a lower energy region was observed for the TiO<sub>2</sub>/SiO<sub>2</sub>, indicating an increase of the band-gap energy in the composite. This finding reaffirms the previous work done by Šuligoj *et al.* [20], who reported that the incorporation of the SiO<sub>2</sub> into the TiO<sub>2</sub> increased its band-gap value, leading to a lower recombination of the charge carriers that contributed to an efficient degradation of the target pollutant.

## 3.1.4. Brunauer-Emmer-Teller (BET) study

**Table 2**

Textural properties of the obtained composites.

| Samples  | Surface area (m <sup>2</sup> /g) | Pore size (nm) | Pore volume (cm <sup>3</sup> /g) |
|--|----------------------------------|----------------|----------------------------------|
| TiO <sub>2</sub>                                       | 46.77                            | 49.16          | 0.21                             |
| TiO <sub>2</sub> /SiO <sub>2</sub>                     | 139.60                           | 31.92          | 0.43                             |
| 1% WO <sub>3</sub> /TiO <sub>2</sub> /SiO <sub>2</sub> | 163.68                           | 24.46          | 0.63                             |
| 3% WO <sub>3</sub> /TiO <sub>2</sub> /SiO <sub>2</sub> | 167.30                           | 22.77          | 0.67                             |
| 5% WO <sub>3</sub> /TiO <sub>2</sub> /SiO <sub>2</sub> | 159.75                           | 26.53          | 0.59                             |
| 7% WO <sub>3</sub> /TiO <sub>2</sub> /SiO <sub>2</sub> | 157.35                           | 26.66          | 0.57                             |

In order to calculate the active surface area and to examine the porous structure of the composite, Table 2 presents the BET surface area, pore size and pore volume values of all the obtained composites. It was found that the TiO<sub>2</sub>/SiO<sub>2</sub> had three times larger surface (139.60 m<sup>2</sup>/g) than that of the TiO<sub>2</sub> (46.77 m<sup>2</sup>/g). This suggests that the addition of SiO<sub>2</sub> into the TiO<sub>2</sub> surface enlarged the surface area of the composites [29].

When the WO<sub>3</sub> was incorporated into the composite, the surface area of the WTS was slightly higher than that of the TiO<sub>2</sub>/SiO<sub>2</sub>. The increase in its surface area not only promoted photocatalytic activity, but also provided additional adsorption sites for the reactants [32-33]. However, the surface area of the WTS composites slightly decreased with the increase in their WO<sub>3</sub> content because an excessive WO<sub>3</sub> blocked the pore diameters, thus reducing the surface area of the composite.

## 3.1.5. SEM analysis

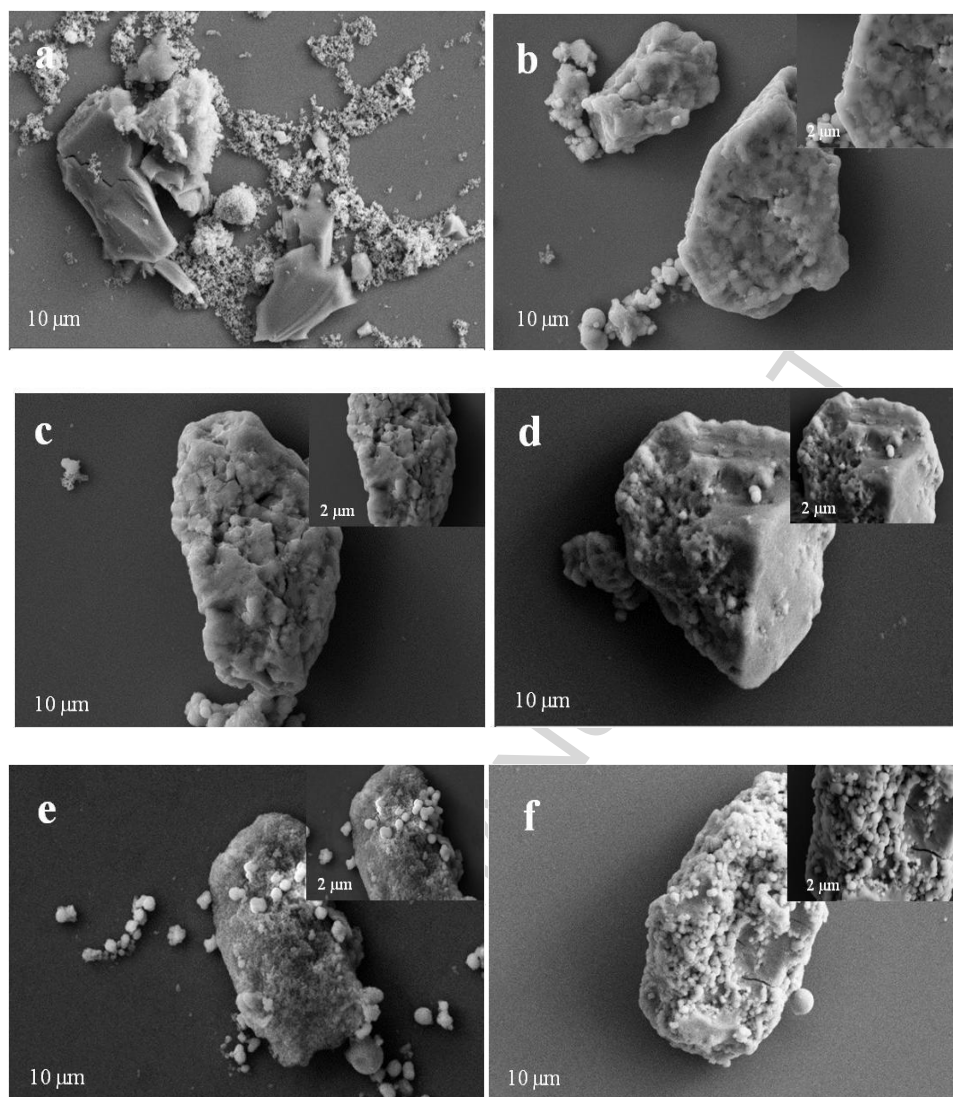


**Fig. 5.** SEM of (a)  $\text{TiO}_2$ , (b)  $\text{TiO}_2/\text{SiO}_2$ , (c) 1% (w/w) of  $\text{WO}_3/\text{TiO}_2/\text{SiO}_2$ , (d) 3% (w/w) of  $\text{WO}_3/\text{TiO}_2/\text{SiO}_2$ , (e) 5% (w/w) of  $\text{WO}_3/\text{TiO}_2/\text{SiO}_2$  and (f) 7% (w/w) of  $\text{WO}_3/\text{TiO}_2/\text{SiO}_2$ .

The morphology of the  $\text{TiO}_2$ ,  $\text{TiO}_2/\text{SiO}_2$  and the synthesized WTS are presented in Fig. 5. As depicted in Fig. 5a, the  $\text{TiO}_2$  are unevenly dispersed and varying in size and shapes, while the surface of the  $\text{TiO}_2/\text{SiO}_2$  (Fig. 5b) is relatively uneven, but agglomerated, providing a larger surface area for promoting the  $\text{WO}_3$  adhesion [34].

In Fig. 5c-5f, all types of the WTS composites exhibited an agglomeration of particles on the surface of the bulk material. Fig. 5 shows that the density of the spherical particles in their surface increased with the increasing ratio of the  $\text{WO}_3$ . The incorporation at different ratios of the  $\text{WO}_3$  into the  $\text{TiO}_2/\text{SiO}_2$  did not damage the mesoporous structure of the  $\text{TiO}_2/\text{SiO}_2$  [31].

When the loading ratio of the  $\text{WO}_3$  reached 7% (w/w), the overall surface of the  $\text{TiO}_2/\text{SiO}_2$  was covered by the  $\text{WO}_3$  particles. Although the  $\text{TiO}_2/\text{SiO}_2$  composite with the  $\text{WO}_3$  improved its surface coverage, this blocked the pores of the  $\text{TiO}_2/\text{SiO}_2$ , thus reducing the active sites for Ace adsorption and leading to its lower removal [35].

### 3.2. Photocatalytic studies

#### 3.2.1. Aqueous systems without light irradiation and/or photocatalysts

The photodegradation of Ace in the absence of both photocatalyst and UV-VIS light irradiation was undertaken. We found that the removal rate was negligible in this preliminary work. To investigate the effects of UV-VIS light irradiation on Ace degradation, blank experiments were carried out without using any photocatalyst. Only 6% of Ace with an initial concentration of 10 mg/L was achieved after 4 h of reaction under the UV-VIS irradiation.

#### 3.2.2. Effects of varying $\text{WO}_3$ contents on the photodegradation efficiency

The WTS photocatalysts containing varying  $\text{WO}_3$  loadings were tested for Ace photodegradation and its results are compared to that of the  $\text{TiO}_2$  and the  $\text{TiO}_2/\text{SiO}_2$  under the same conditions. Fig. 6 presents an Ace photodegradation efficiency using all the obtained composites with an initial concentration of 10 mg/L.

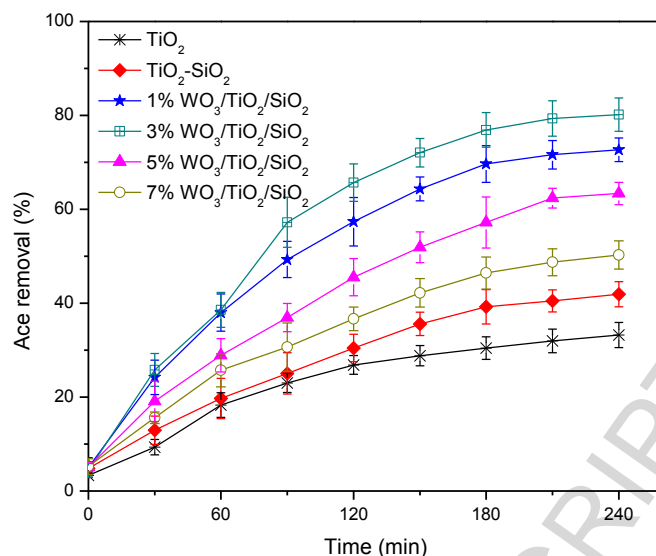


**Fig. 6.** Photodegradation rate of Ace on TiO<sub>2</sub>, TiO<sub>2</sub>/SiO<sub>2</sub> and various WO<sub>3</sub> loading ratios in WO<sub>3</sub>/TiO<sub>2</sub>/SiO<sub>2</sub> photocatalysts (10 mg/L of Ace; 1.0 g/L of photocatalysts; pH: 9; 25°C; 4 h).

Under the same concentration of 10 mg/L, the Ace removal by the TiO<sub>2</sub>/SiO<sub>2</sub> composite (42%) was higher than that of the TiO<sub>2</sub> alone (33%). This suggests that the TiO<sub>2</sub>/SiO<sub>2</sub> was capable of utilizing the visible light more effectively than that of the pure TiO<sub>2</sub>, as reflected by the DRS UV-VIS analyses (Fig. 4). In addition, the incorporation of the SiO<sub>2</sub> provided additional sites, as indicated by the SEM results [31]. This was attributed to the increasing surface area after being loaded with the WO<sub>3</sub> (Table 2).

In addition, the incorporation of the WO<sub>3</sub> in the composite promoted a higher affinity for chemical species with unpaired electrons due to Lewis acidity [31]. The results reveal that the removal rate of Ace significantly increased from 42% to 80% at the same Ace concentration of 10 mg/L upon the increasing WO<sub>3</sub> ratios to 3% (w/w). When the loading ratio of WO<sub>3</sub> reached 7% (w/w), the removal rate of Ace decreased to 50%. Overall, the 3% (w/w) of WTS photocatalyst exhibited the highest photocatalytic activity among those composites.

The photodegradation rate of Ace during the photocatalytic reaction can be represented by the following pseudo-first order reaction:

$$\ln(\eta_e - \eta_t) = \ln(\eta_e) - kt/2.303 \quad (3)$$

where  $k$  ( $\text{h}^{-1}$ ) is the first order rate constant of Ace removal, while  $\eta_e$  and  $\eta_t$  (%) represent the removal of Ace by photocatalysts at equilibrium and at a given time, respectively.

Fig. 7 presents the pseudo-first order fitting curves with the  $\text{TiO}_2$ , the  $\text{TiO}_2/\text{SiO}_2$  and with varying WTS photocatalysts. Their rate constants ( $k$ ) are presented in Table 3. The table suggests that the kinetics of all the synthesized composites for the photodegradation of Ace followed the pseudo-first order kinetics based on their correlation coefficients ( $R^2$ ).

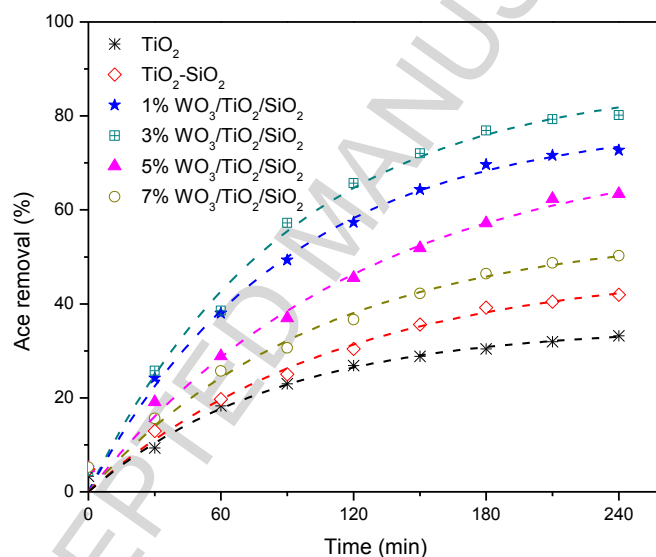


**Fig. 7.** Plots of Ace removal over irradiation time with  $\text{TiO}_2$ ,  $\text{TiO}_2/\text{SiO}_2$  and various  $\text{WO}_3$  loading ratios in  $\text{WO}_3/\text{TiO}_2/\text{SiO}_2$  composites

**Table 3**

Summary of degradation rates of various photocatalysts for Ace removal.

| Samples  | $\eta_e$ (%) | $k$ ( $\text{h}^{-1}$ ) | $R^2$  |
|--|--------------|-------------------------|--------|
| TiO <sub>2</sub>                                       | 35           | 0.49                    | 0.9833 |
| TiO <sub>2</sub> /SiO <sub>2</sub>                     | 56           | 0.53                    | 0.9753 |
| 1% WO <sub>3</sub> /TiO <sub>2</sub> /SiO <sub>2</sub> | 79           | 0.67                    | 0.9917 |
| 3% WO <sub>3</sub> /TiO <sub>2</sub> /SiO <sub>2</sub> | 88           | 0.70                    | 0.9910 |
| 5% WO <sub>3</sub> /TiO <sub>2</sub> /SiO <sub>2</sub> | 75           | 0.66                    | 0.9858 |
| 7% WO <sub>3</sub> /TiO <sub>2</sub> /SiO <sub>2</sub> | 56           | 0.57                    | 0.9833 |

Among all the obtained photocatalysts, the 3% (w/w) of WTS composite presented the highest constant rate ( $0.70 \text{ h}^{-1}$ ). This suggests that the photodegradation rate of Ace using 3% (w/w) WTS was faster than that using the TiO<sub>2</sub>, the TiO<sub>2</sub>/SiO<sub>2</sub> or the other WTS composites.

### 3.3. Effects of initial concentration on Ace photodegradation

An effective removal of target pollutants requires an optimum concentration during the photodegradation. Therefore, it is important to determine the optimum concentration of Ace. Fig. 8 presents an Ace removal efficiency (%) versus the degradation time with its varying concentrations from 5 to 25 mg/L.

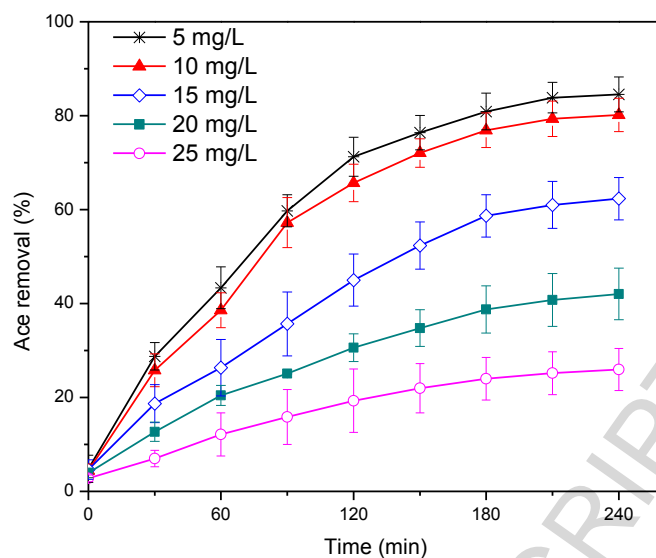
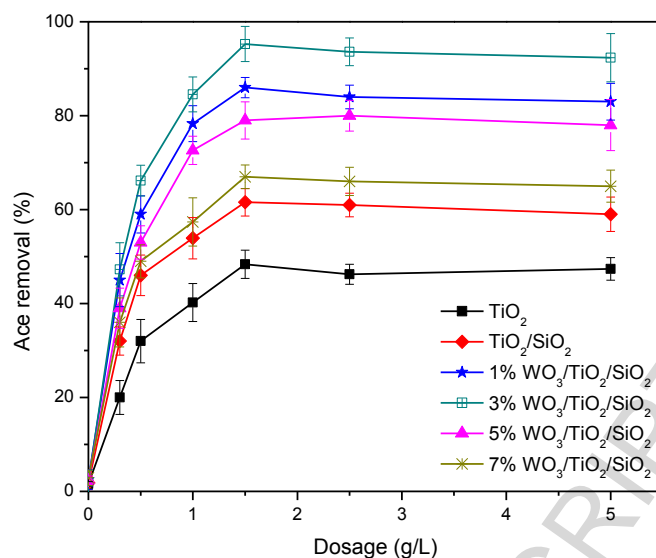


**Fig. 8.** Effects of initial concentration on the photodegradation of Ace (1.0 g/L of 3% (w/w)  $\text{WO}_3/\text{TiO}_2/\text{SiO}_2$ ; pH: 9;  $25^\circ\text{C}$ ; 4 h).

When the Ace concentration increased from 5 to 25 mg/L, the photodegradation rate of Ace decreased from 85% to 26%. Increasing the Ace concentration would accelerate the formation of the adsorption layer by the photocatalyst as reported by Kurniawan *et al.* [13]. As the initial concentration of Ace increased, the adsorption layer became thicker, thus preventing the photon from the UV-VIS light source from reaching the surface of the photocatalyst. As a result, the adsorption of Ace onto the surface of the photocatalyst was limited, thus lowering the removal of Ace.

#### 3.4. Effects of dosage of photocatalysts on Ace photodegradation

In order to study the effects of dose of photocatalyst on the Ace removal, a series of Ace photodegradation experiments was carried out by using 3% (w/w) of WTS at an Ace concentration of 5 mg/L. The experiments were performed at varying dosage from 0.3 g/L to 1.5 g/L.



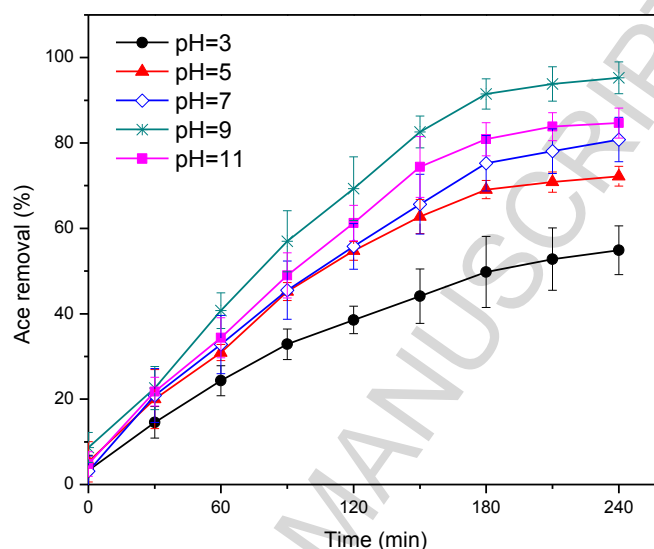
**Fig. 9.** Effects of the dosage of the photocatalyst (5 mg/L of Ace; pH: 9; 25°C; 4 h).

Fig. 9 demonstrates changes in Ace removal with the varying photocatalysts dosages. The Ace removal improved with the increasing photocatalysts dosage from 0.3 g/L to 1.5 g/L. This might be due to the fact that the higher is the dose of the photocatalyst, the greater is the availability of the active sites for the Ace adsorption.

Further increase in the dose of the photocatalyst beyond 1.5 g/L resulted in a decreasing Ace removal. This could be explained due to the fact that the interaction of the Ace molecules with the photocatalysts would aggregate into clusters when it is overdosed, thus decreasing the numbers of the active sites on the surface of the WTS composite and shielding the UV-VIS light from reaching the surface of the photocatalyst. Consequently, it reduced the generation of  $\cdot\text{OH}$  during the photocatalytic treatment [36]. Overall, 1.5 g/L was chosen as the optimum dose for Ace degradation. However, the treated effluents still could not meet the increasingly strict requirements set by China and the US legislations of less than 0.2 mg/L in this study [37].

### 3.5. Effects of pH on the photocatalytic performance

Optimum pH in photodegradation reaction is important since this affects both the charge properties of the surface of photocatalyst and the electrostatic interactions between a photocatalyst and target pollutant [29, 38, 39]. The experiments were carried out at optimized conditions with varying pH from 3 to 11 (Fig. 10).



**Fig. 10.** Effects of pH on Ace photodegradation rate (5 mg/L of Ace; 1.5 g/L of 3% (w/w)  $\text{WO}_3/\text{TiO}_2/\text{SiO}_2$ ; 25°C; 4 h).

With the increasing pH, the Ace removal gradually increased and reached its maximum removal at pH 9 (95%) with an initial Ace concentration of 5 mg/L. When pH ranged between 6.5 and 9.5, the surface of the photocatalyst became negatively charged (with a  $\text{pH}_{\text{zpc}}$  6.4) [40], promoting electrostatic attractions with the positively charged Ace molecules (with a  $\text{pK}_a$  of 9.5) [41]. When the solution pH reached 11, the Ace removal slightly decreased to 80%. Since both the 3WTS composite and the Ace molecules were negatively charged, the photocatalyst was electrostatically repelled to the negatively charged Ace molecules, resulting in a lower Ace removal. This result suggests that alkaline conditions are favorable for the photocatalytic degradation of Ace by the 3WTS composite.

## 3.6. Proposed mechanisms and photodegradation pathways of Ace removal

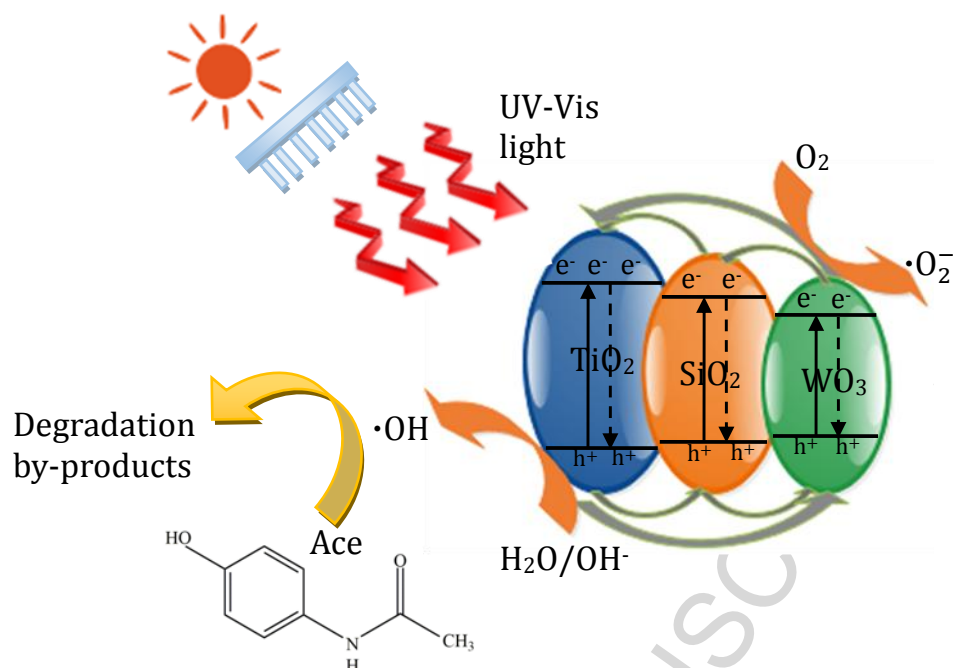
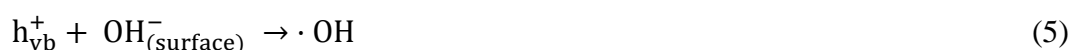


**Fig. 11.** Scheme of photocatalytic degradation of Ace by  $\text{WO}_3/\text{TiO}_2/\text{SiO}_2$ .

Fig. 11 describes a scheme of the Ace photodegradation mechanisms by the WTS. It is known that  $h_{vB}^+$  and  $e_{cB}^-$  are important due to their roles in generating  $\cdot\text{OH}$  and  $\cdot\text{O}_2^-$  [42]. The electron-hole pairs on the surface of photocatalysts are formed through photo-excitation (Reaction (4)). Afterward, the  $e_{cB}^-$  in the conduction band reacts with  $\text{O}_2$  (Reaction 5). The  $h_{vB}^+$  in the valence band, trapped by the  $\text{OH}^-$  on its surface, generates  $\cdot\text{OH}$  to oxidize the target contaminant (Reactions (4)-(10)) [29].





Possible reaction pathways of Ace photodegradation by the WTS composite are presented in Fig. 12. Hydroxylation and photolysis processes represent initial steps, where  $\cdot\text{OH}$  attacked the *ortho*- or *para*- of the Ace's aromatic ring. The oxidation by-products include hydroquinone and 1,4-benzoquinone [43].

ACCEPTED MANUSCRIPT



### 3.7. Reuse of spent $WO_3/TiO_2/SiO_2$ photocatalyst

Regeneration of a photocatalyst that enables it to maintain its photocatalytic activity for subsequent use without changing its original chemical structure is important for water technology. Fig. 13 presents the regeneration efficiency of the spent 3WTS (3% (w/w)). The spent 3WTS still remained stable after being regenerated for four consecutive times without significant changes with respect to its removal capacities. As indicated in Fig. 11, the photodegradation rate of Ace by the spent 3WTS was still 82% under the same concentration of 5 mg/L. This indicates that the 3% (w/w) of WTS photocatalyst was promising for practical applications.

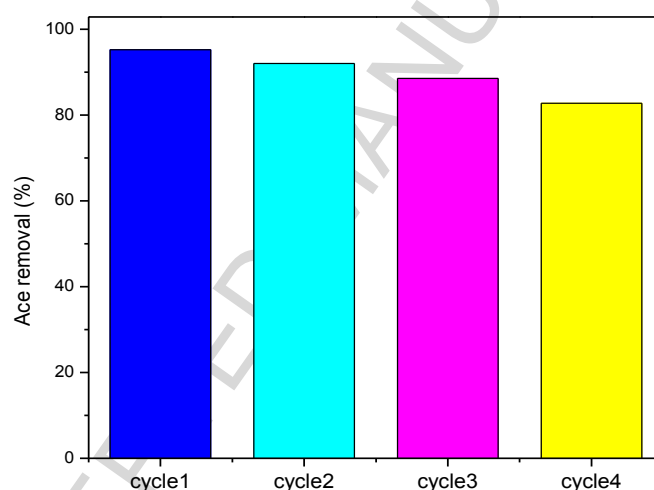


**Fig. 13.** Reusability of spent 3% (w/w) of  $WO_3/TiO_2/SiO_2$  composite on Ace removal (5 mg/L of Ace; 1.5 g/L of 3% (w/w)  $WO_3/TiO_2/SiO_2$ ; pH 9.0; 25°C; 4 h).

### 3.8. Comparison of photodegradation performance among various photocatalysts

In order to evaluate the photocatalytic performance of the WTS composite in this study, a comparative study is presented in terms of photocatalyst dosage (g/L), concentration (mg/L), light sources, pH and removal efficiency. Table 4 summarizes the photocatalytic

degradation of organic pollutants in previous studies. Although this comparison has a relative meaning due to varying operating conditions (dose (g/L), light sources, energy (W), reaction time (min) and pH), this comparison is still useful to evaluate the overall performance of those photocatalysts for water treatment applications.

Table 4 shows that semiconductor materials such as  $\text{TiO}_2$ ,  $\text{SiO}_2$ ,  $\text{WO}_3$  and  $\text{ZnO}$  present outstanding performances among the various photocatalysts. As for contaminants like endocrine-disrupting compounds (EDC) or PPCPs, Hunge *et al.* [44] found that only 65% removal of 4-chlorophenol was achieved after 3 h with an initial concentration of 25 mg/L [44], while Yan *et al.* [45] achieved 95% of Ace removal using  $\text{In}_2\text{S}_3/\text{Zn}_2\text{GeO}_4$  with its initial concentration of 5 mg/L. Although various photocatalysts can be applied, key factors in the selection of wastewater treatment containing PPCPs are its photocatalytic activity and the pollutants' removal rate. The reaction time, pH and the required intensity of UV-VIS light irradiation that affect the removal efficiency depend on the concentration of target pollutants and the type of semiconductor materials.

**Table 4**

Summary of photocatalytic performance of various photocatalysts.

| Target pollutant  | Initial concentration (mg/L) | Type of photocatalysts   | Dosage (g/L) | Light sources    | Energy (W) | Time (min) | pH              | Removal efficiency (%) | References    |
|-------------------|------------------------------|--|--------------|------------------|------------|------------|-----------------|------------------------|---------------|
| imazapyr          | 20                           | TiO <sub>2</sub> /WO <sub>3</sub>                                  | 1            | LED lamp         | NA         | 120        | 4               | 100                    | [31]          |
| bromocresol green | 10                           | Fe <sub>3</sub> O <sub>4</sub> /SiO <sub>2</sub> /TiO <sub>2</sub> | 0.25         | UV lamp          | NA         | 180        | 3.7             | 100                    | [46]          |
| Ace               | 5                            | GR-TNT <sup>h</sup>  | 0.1          | UV lamp          | 14         | 180        | NA              | 96                     | [38]          |
| Ace               | 5                            | WO <sub>3</sub> /TiO <sub>2</sub> /SiO <sub>2</sub>                | 1.5          | Xenon lamp       | 500        | 240        | 9               | 95                     | Present study |
| Ace               | 5                            | In <sub>2</sub> S <sub>3</sub> /Zn <sub>2</sub> GeO <sub>4</sub>   | 1            | Xenon lamp       | NA         | 360        | NA              | 95                     | [45]          |
| Ace               | 15                           | C-doped <sup>i</sup> TiO <sub>2</sub>                              | 1            | Five LED lamp    | 1          | 500        | 6.9             | 94                     | [47]          |
| RhB <sup>a</sup>  | 10                           | TiO <sub>2</sub> /SiO <sub>2</sub> NF <sub>s</sub> <sup>b</sup>    | 0.2          | ultraviolet lamp | 25         | 90         | NA <sup>c</sup> | 91                     | [48]          |
| MO <sup>d</sup>   | 100                          | TiO <sub>2</sub> /SiO <sub>2</sub>                                 | 2.5          | Hg UV lamp       | 175        | 120        | 8               | 95                     | [29]          |
| MA <sup>f</sup>   | 250                          | ZnO-CuO NCP <sup>g</sup>   | 0.1          | Hg lamp          | 55         | 200        | 5.6             | 70                     | [49]          |
| 4-CP <sup>e</sup> | 25                           | TiO <sub>2</sub> /WO <sub>3</sub>                                  | 1.2          | sunlight         | NA         | 180        | 7               | 65                     | [44]          |

a RhB: rhodamine B

b NF<sub>s</sub>: nanofibers

c NA: not available

---

d MO: methyl orange

e 4-CP: 4-chlorpphenol

f MA: mefenamic acid

g NCP: clinoptilolite nanoparticles

h GR-TNT: Graphene-Titanium dioxide nanotube

i C-dropped: carbon self-dropped

ACCEPTED MANUSCRIPT

#### 4. Conclusions

This study has demonstrated that the incorporation of the  $\text{WO}_3$  into the  $\text{TiO}_2/\text{SiO}_2$  composite has significantly enhanced the photocatalytic degradation of Ace from synthetic wastewater under the UV-VIS irradiation. Under optimized conditions (1.5 g/L of 3% (w/w) of  $\text{WO}_3/\text{TiO}_2/\text{SiO}_2$  composite, pH 9 and 4 h of reaction time), 95% of Ace removal could be achieved at the same 5 mg/L of initial Ace concentration. Under those same conditions, the result of Ace photodegradation by the 3% (w/w) of the  $\text{WO}_3/\text{TiO}_2/\text{SiO}_2$  composite was significantly higher (95%) than that by the individual  $\text{TiO}_2/\text{SiO}_2$  (42%) and/or the  $\text{TiO}_2$  alone (33%). It is important to note that the treated effluents still could not meet the maximum limit of less than 0.2 mg/L set by China's and US legislation. This indicates that further subsequent treatment like biological processes is still necessary for completing the removal of target pollutant from wastewater samples.

#### Acknowledgements

The authors express their profound gratitude to the Xiamen University's Foundation of Technology for the research grant No. 20720150070.

**References**

- [1] G. Zhang, Y. Sun, C. Zhang, Z. Yu, Decomposition of acetaminophen in water by a gas phase dielectric barrier discharge plasma combined with TiO<sub>2</sub>-rGO nanocomposite: Mechanism and degradation pathway, *J. Hazard. Mater.* 323 (2017) 719-729.
- [2] T.A. Kurniawan, W. Lo, G. Chan, M. Sillanpaa, Biological processes for treatment of landfill leachate, *J. Environ. Monit.* 12(11) (2010) 2032-2047.
- [3] A. Peng, M. Huang, Z. Chen, C. Gu, Oxidative coupling of acetaminophen mediated by Fe<sup>3+</sup>-saturated montmorillonite, *Sci. Total Environ.* 595 (2017) 673-680.
- [4] Q. Sun, M. Lv, A. Hu, X. Yang, C.P. Yu, Seasonal variation in the occurrence and removal of pharmaceuticals and personal care products in a wastewater treatment plant in Xiamen, China, *J. Hazard. Mater.* 277 (2014) 69-75.
- [5] A. Durán, J.M. Monteagudo, A. Carnicer, M. Ruiz-Murillo, Photo-Fenton mineralization of synthetic municipal wastewater effluent containing acetaminophen in a pilot plant, *Desalination.* 270 (2011) 124-129.
- [6] S. Ba, L. Haroune, C.C. Morató, C. Jacquet, I.E. Touahar, J.P. Bellenger, C.Y. Legault, J.P. Jones, H. Cabana, Synthesis and characterization of combined cross-linked laccase and tyrosinase aggregates transforming acetaminophen as a model phenolic compound in wastewater, *Sci. Total Environ.* 487 (2014) 748-755.
- [7] N. Abdullah, M.A. Fulazzaky, E.L. Yong, A. Yuzir, P. Sallis, Assessing the treatment of acetaminophen-contaminated brewery wastewater by an anaerobic packed-bed reactor, *J. Environ. Manage.* 168 (2016) 273-279.
- [8] G. Moussavi, H. Momeninejad, S. Shekoohiyan, P. Baratpour, Oxidation of acetaminophen in the contaminated water using UVC/S<sub>2</sub>O<sub>8</sub><sup>2-</sup> process in a cylindrical photoreactor: Efficiency and kinetics of degradation and mineralization, *Sep. Purif. Technol.* 181 (2017) 132-138.

- [9] S. Esplugas, D.M. Bila, L.G.T. Krause, M. Dezotti, Ozonation and advanced oxidation technologies to remove endocrine disrupting chemicals (EDCs) and pharmaceuticals and personal care products (PPCPs) in water effluents, *J. Hazard. Mater.* 149 (2007) 631-642.
- [10] T.A. Kurniawan, W.H. LO, Removal of refractory compounds from stabilized landfill leachate using an integrated H<sub>2</sub>O<sub>2</sub> oxidation and granular activated carbon adsorption treatment, *Water Res.* 43 (2009) 4079-4091.
- [11] T.A. Kurniawan, W.H. LO, G. Chan., Radicals-catalyzed oxidation for degradation of recalcitrant compounds from landfill leachate, *Chem Eng J.* 125 (2006) 35-57.
- [12] W. Lin, H. Zheng, P. Zhang, T. Xu, Pt deposited TiO<sub>2</sub> films with exposed facets for photocatalytic degradation of a pharmaceutical pollutant, *Appl Catal A-Gen.* 521 (2016) 75-82.
- [13] T.A. Kurniawan, L. Yanyan, T. Ouyang, A. Albadarin, G. Walker, BaTiO<sub>3</sub>/TiO<sub>2</sub> composite-assisted photocatalytic degradation for removal of acetaminophen from synthetic wastewater under UV-VIS Irradiation, *Mater. Sci. Semicond. Proc.*  
DOI <https://doi.org/10.1016/j.mssp.2017.06.048>(2017).
- [14] D. Zhang, J. Wu, B. Zhou, Y. Hong, S. Lia, W. Wen, Efficient photocatalytic activity with carbon-doped SiO<sub>2</sub> nanoparticles, *Nanoscale* 5 (2013) 6167-6172.
- [15] S. Murgolo, F. Petronella, R. Ciannarella, R. Comparelli, A. Agostiano, M.L. Curri, G. Mascolo, UV and solar-based photocatalytic degradation of organic pollutants by nano-sized TiO<sub>2</sub> grown on carbon nanotubes, *Catal. Today* 240, Part A (2015) 114-124.
- [16] S.P. Adhikari, H. Dean, Z.D. Hood, R. Peng, K.L. More, I. Ivanov, Z. Wu, A. Lachgar, Visible-light-driven Bi<sub>2</sub>O<sub>3</sub>/WO<sub>3</sub> composites with enhanced photocatalytic activity, *RSC Adv.* 5 (2015) 91094-91102.
- [17] D. Wang, H. Yu, Y. Zhu, C. Song, NiO nanosheets rooting into Ni-doped CeO<sub>2</sub>

- microspheres for high performance of CO catalytic oxidation, *Maters. Lett.* 198 (2017) 168-171.
- [18] Y. Zeng, T. Wang, S. Zhang, Y. Wang, Q. Zhong, Sol-gel synthesis of CuO-TiO<sub>2</sub> catalyst with high dispersion CuO species for selective catalytic oxidation of NO, *Appl. Surf. Sci.* 411 (2017) 227-234.
- [19] N. Devnarain, C. Tiloke, S. Nagiah, A.A. Chuturgoon, Fusaric acid induces oxidative stress and apoptosis in human cancerous oesophageal SNO cells, *Toxicol.* 126 (2017) 4-11.
- [20] A. Šuligoj, U.L. Štangar, A. Ristić, M. Mazaj, D. Verhovšek, N.N. Tušar, TiO<sub>2</sub>-SiO<sub>2</sub> films from organic-free colloidal TiO<sub>2</sub> anatase nanoparticles as photocatalyst for removal of volatile organic compounds from indoor air, *Appl. Catal. B-Environ.* 184 (2016) 119-131.
- [21] S. Qourzal, N. Barka, M. Tamimi, A. Assabbane, A. Nounah, A. Ihlal, Y. Ait-Ichou, Sol-gel synthesis of TiO<sub>2</sub>-SiO<sub>2</sub> photocatalyst for β-naphthol photodegradation, *Maters. Sci. Eng., C.* 29 (2009) 1616-1620.
- [22] Z. Fang, T. Lin, H. Xu, G. Wu, M. Sun, Y. Chen, Novel promoting effects of cerium on the activities of NO<sub>x</sub> reduction by NH<sub>3</sub> over TiO<sub>2</sub>-SiO<sub>2</sub>-WO<sub>3</sub> monolith catalysts, *J. Rare Earth.* 32 (2014) 952-959.
- [23] H.I.V. Vidales, A. Jiménez-González, A. Bautista-Orozco, C.A. Arancibia-Bulnes, C.A. Estrada, Solar production of WO<sub>3</sub>: a green approach, *Green Proc. Synth.* 4(2015) 167-177.
- [24] Y.M. Hunge, Sunlight assisted photoelectrocatalytic degradation of benzoic acid using stratified WO<sub>3</sub>/TiO<sub>2</sub> thin films, *Ceram. Int.* 43 (2017) 10089-10096.
- [25] F. Riboni, M.V. Dozzi, M.C. Paganini, E. Giamello, E. Selli, Photocatalytic activity of TiO<sub>2</sub>-WO<sub>3</sub> mixed oxides in formic acid oxidation, *Catal. Today* 287 (2017) 176-181.
- [26] T.A. Kurniawan, M.Sillanpaa, Nano-adsorbents for remediation of aquatic environment: local solutions to global pollution problems, *Crit. Rev. Env. Sci. Technol.* 42 (2012) 1233-1295.
- [27] K.P.O. Mahesh, D.H. Kuo, Synthesis of Ni nanoparticles decorated SiO<sub>2</sub>/TiO<sub>2</sub> magnetic

spheres for enhanced photocatalytic activity towards the degradation of azo dye, *Appl. Surf. Sci.* 357 (2015) 433-438.

[28] M. Nasirian, C.F. Bustillo-Lecompte, M. Mehrvar, Photocatalytic efficiency of Fe<sub>2</sub>O<sub>3</sub>/TiO<sub>2</sub> for the degradation of typical dyes in textile industries: Effects of calcination temperature and UV-assisted thermal synthesis, *J. Environ. Manage.* 196 (2017) 487-498.

[29] N. Guo, Y. Liang, S. Lan, L. Liu, G. Ji, S. Gan, H. Zou, X. Xu, Uniform TiO<sub>2</sub>-SiO<sub>2</sub> hollow nanospheres: Synthesis, characterization and enhanced adsorption-photodegradation of azo dyes and phenol, *Appl. Surf. Sci.* 305 (2014) 562-574.

[30] C. Ren, W. Qiu, Y. Chen, Physicochemical properties and photocatalytic activity of the TiO<sub>2</sub>/SiO<sub>2</sub> prepared by precipitation method, *Sep. Purif. Technol.* 107 (2013) 264-272.

[31] A.A. Ismail, I. Abdelfattah, A. Helal, S.A. Al-Sayari, L. Robben, D.W. Bahnemann, Ease synthesis of mesoporous WO<sub>3</sub>-TiO<sub>2</sub> nanocomposites with enhanced photocatalytic performance for photodegradation of herbicide imazapyr under visible light and UV illumination, *J. Hazard. Mater.* 307 (2016) 43-54.

[32] G. Liao, S. Chen, X. Quan, Y. Zhang, H. Zhao, Remarkable improvement of visible light photocatalysis with PANI modified core-shell mesoporous TiO<sub>2</sub> microspheres, *Appl. Catal. B-Environ.* 102 (2011) 126-131.

[33] A.A. Ismail, D.W. Bahnemann, Mesoporous titania photocatalysts: preparation, characterization and reaction mechanisms, *J. Mater. Chem.* 21 (2011) 11686-11707.

[34] C.S. Kim, J.W. Shin, S.H. An, H.D. Jang, T.O. Kim, Photodegradation of volatile organic compounds using zirconium-doped TiO<sub>2</sub>/SiO<sub>2</sub> visible light photocatalysts, *Chem. Eng. J.* 204 (2012) 40-47.

[35] T.A. Kurniawan, W.H. Lo, E. Repo, M. Sillanpaa, Removal of 4-chlorophenol from contaminated water using coconut shell waste pretreated with chemical agents, *J. Chem. Technol.*

Biotechnol. 85 (2010) 1616-1627.

[36] S. Kappadan, T.W. Gebreab, S. Thomas, N. Kalarikkal, Tetragonal BaTiO<sub>3</sub> nanoparticles: An efficient photocatalyst for the degradation of organic pollutants, Mater. Sci. Semicond. Proc. 51 (2016) 42-47.

[37] MDH, Toxicological Summary for: Acetaminophen, Minnesota Department of Health, 2015

[38] H. Tao, X. Liang, Q. Zhang, C.T. Chang, Enhanced photoactivity of graphene/titanium dioxide nanotubes for removal of Acetaminophen, Appl. Surf. Sci. 324 (2015) 258-264.

[39] S. Babel, T.A. Kurniawan, Cr(VI) removal from synthetic wastewater using coconut shell charcoal and commercial activated carbon modified with oxidizing agents and/or chitosan, Chemosphere 54 (2004) 951-967.

[40] X.Z. Li, F.B. Li, C.L. Yang, W.K. Ge, Photocatalytic activity of WO<sub>x</sub>-TiO<sub>2</sub> under visible light irradiation, J. Photochem. Photobiol. A. 141 (2001) 209-217.

[41] C.T. Chang, J.J. Wang, T. Ouyang, Q. Zhang, Y.H. Jing, Photocatalytic degradation of acetaminophen in aqueous solutions by TiO<sub>2</sub>/ZSM-5 zeolite with low energy irradiation, Mater. Sci. Eng., B. 196 (2015) 53-60.

[42] X. Cheng, X. Yu, Z. Xing, Characterization and mechanism analysis of N doped TiO<sub>2</sub> with visible light response and its enhanced visible activity, Appl. Surf. Sci. 258 (2012) 3244-3248.

[43] C.A. Aguilar, C. Montalvo, J.G. Ceron, E. Moctezuma, Photocatalytic degradation of acetaminophen, Int. J. Environ. Res. 5 (2011) 1071-1078.

[44] Y.M. Hunge, M.A. Mahadik, A.V. Moholkar, C.H. Bhosale, Photoelectrocatalytic degradation of oxalic acid using WO<sub>3</sub> and stratified WO<sub>3</sub>/TiO<sub>2</sub> photocatalysts under sunlight illumination, Ultrason. Sonochem. 35 (2017) 233-24.

[45] T. Yan, T. Wu, Y. Zhang, M. Sun, X. Wang, Q. Wei, B. Du, Fabrication of In<sub>2</sub>S<sub>3</sub>/Zn<sub>2</sub>GeO<sub>4</sub>

composite photocatalyst for degradation of acetaminophen under visible light, *J. Coll. Int. Sci.*

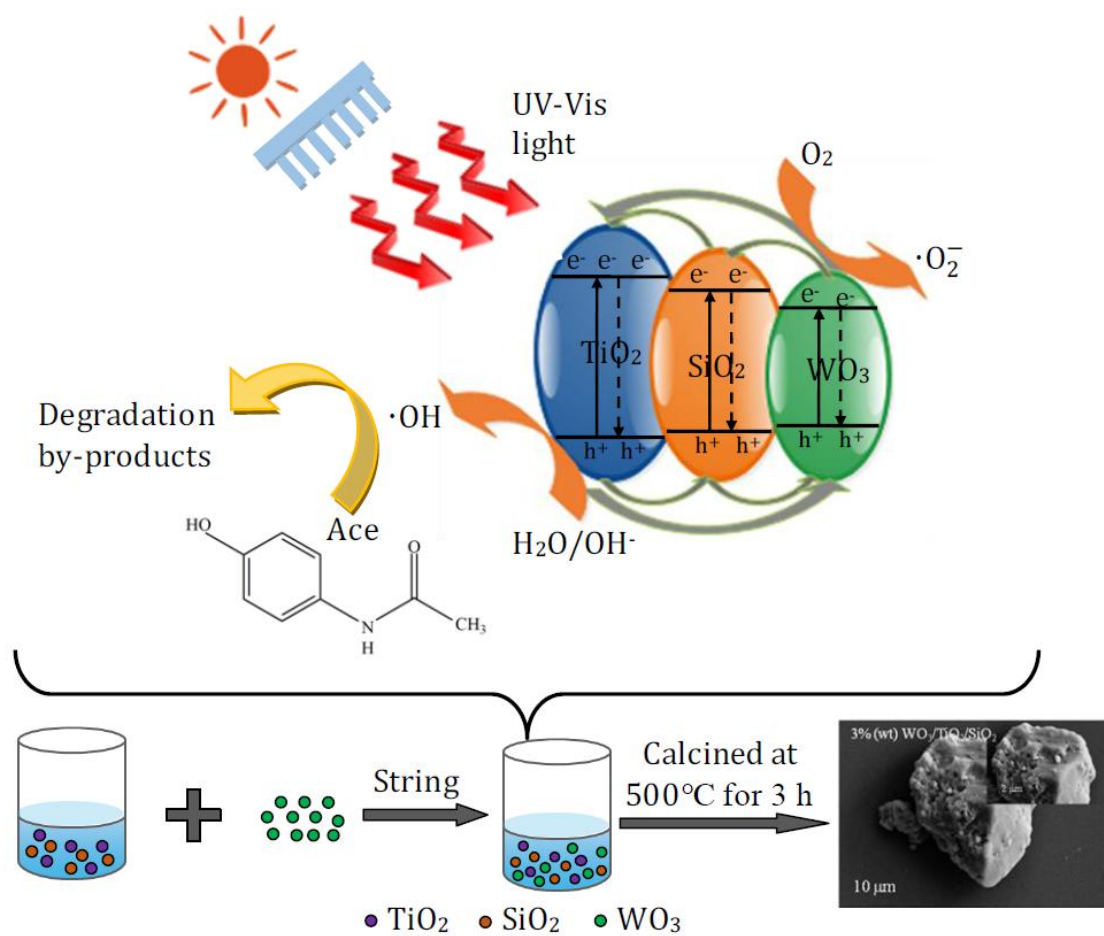
DOI <https://doi.org/10.1016/j.jcis.2017.06.079>.

[46] L.E. Ahangar, K. Movassaghi, M. Emadi, F. Yaghoobi, Photocatalytic application of TiO<sub>2</sub>/SiO<sub>2</sub>-based magnetic nanocomposite (Fe<sub>3</sub>O<sub>4</sub>@SiO<sub>2</sub>/TiO<sub>2</sub>) for reusing of textile wastewater, *Nanochem. Res.* 1 (2016) 33-39.

[47] M.D.G. de Luna, J.C.T. Lin, M.J.N. Gotostos, M.C. Lu, Photocatalytic oxidation of acetaminophen using carbon self-doped titanium dioxide, *Sust. Environ Res.* 26 (2016) 161-167.

[48] X. Tang, Q. Feng, K. Liu, T. Yan, Synthesis and characterization of a novel nanofibrous TiO<sub>2</sub>/SiO<sub>2</sub> composite with enhanced photocatalytic activity, *Maters. Letts.* 183 (2016) 175-178.

[49] A. Shirzadi, A.N. Ejhieh, Enhanced photocatalytic activity of supported CuO–ZnO semiconductors towards the photodegradation of mefenamic acid aqueous solution as a semi real sample, *J. Mol. Catal. A-Chem.* 411 (2016) 222-229.



Graphical abstract

### Highlights

1. The  $\text{WO}_3/\text{SiO}_2/\text{TiO}_2$  is a promising composite for acetaminophen photodegradation;
2. The WTS composite has stable characteristics;
3. The spent composite could be regenerated with stable removal efficiency of Ace.

ACCEPTED MANUSCRIPT